BIOORGANIC CHEMISTRY 16, 376–387 (1988)

Conformational Flexibility in the Molecular Structure of Rotenone, a Naturally Occurring Insecticide

M. ROSSI,*,[1] P. Z. FULE,* AND M. R. TAYLOR†

*Department of Chemistry, Vassar College, Poughkeepsie, New York 12601, and
†School of Physical Sciences, The Flinders University of South Australia, Bedford Park, South Australia 5042, Australia

Received October 14, 1987

The crystal and molecular structure of rotenone, a naturally occurring insecticide with mitochondrial and mitotic spindle inhibitory properties, was determined by direct methods. The crystals were orthorhombic, space group, $P2_12_12_1$ with two molecules in the asymmetric unit; $a = 8.413$ (1) Å, $b = 19.840(1)$, $c = 23.581(1)$, $V = 3936$ Å^3, $Z = 8$. The structure was refined by least-squares methods to a final $R = 0.067$. The two molecules in the asymmetric unit have different conformations about the junction between the nonaromatic rings **B** and **C**. Ring **B** is in a sofa conformation in both molecules, with a slight distortion toward a half-chair in **I**, but with C8 and C8′ on opposite sides of the planar part of the rings. This difference in conformation results in **I** having an extended (linear) shape while **II** is V-shaped. The more elongated conformation of the molecule **(I)** has not been reported in previous studies. Ring C also has opposite conformations in the two molecules. The angle between the planes formed by rings **A** and **D** in molecule **I** is 64.3°, while in molecule **II** it is 88.3°. Molecular mechanics techniques were used to determine the energy of the two conformations. These calculations, at room temperature, predict molecule **II** to be the more stable conformer. The highly flexible site in the **B/C** ring junction is also chemically very reactive. This flexibility and reactivity are further discussed in terms of rotenone's inhibitory activities.

INTRODUCTION

Rotenone is a naturally occurring heterocyclic compound with inhibitory effects on oxidative phosphorylation and mitosis. It is obtained from the roots of the legumes *Derris elliptica* and *D. malaccensis* in Malaysia and *D. Uruco* and *Lonchocarpus utilis* in South America (*1, 2*). Rotenone is a widely used pesticide (*3–5*); together with other botanical pesticides (e.g., pyrethrum, sabadilla, nicotine, and ryania), it is a valuable alternative to the synthetic pesticides in use today. These latter substances act as neurotoxicants by inhibiting insect cholinesterase at nerve synapses, leading to paralysis and death (*1, 2, 6*). Some insects have developed a resistance in response to the heavy use of these pesticides. In contrast, the botanicals exert their action through a variety of biochemical lesions and therefore can control neurotoxicant resistant insects. Additionally, as naturally occurring substances the botanicals appear to be metabolized to less toxic derivatives. For

[1] To whom correspondence should be addressed.

0045-2068/88 $3.00

rotenone, these are the polar rotenolones and hydroxyrotenones (*7*). It photochemically decomposes to form over 20 degradation products, including rotenoids, rotenolones, rotenononone, and their expoxides (*3–9*).

Rotenone is biochemically very active (*10–15*), exerting its effects mainly by blocking oxidative phosphorylation and/or mitosis in cells through apparently separate pathways (*10*). Experimental evidence has located the site of rotenone inhibition of oxidative phosphorylation in the electron transport particles of the mitochondrion (*16–18*). Rotenone inhibits NADH dehydrogenase, the enzyme which oxidizes the reduced form of nicotinamide adenine dinucleotide at complex **I** in the oxidative phosphorylation chain, on the O_2 side of the enzyme (*16–18*). The binding site appears to be noncovalent and to involve both lipid and protein (*16*). Further, in mammals, rotenone appears to act by causing a conformational change in the enzyme (complex **I**) upon its binding, thereby making the seven protein subunits of complex **I** move away from each other (*19*) and preventing reduction of ubiquinone, the natural substrate.

Rotenone inhibits tubulin self-assembly and, thus, mitosis (*10, 20*). The nature of this inhibition (*21*) is such that rotenone does not act by breaking down tubulin aggregates, nor by modifying protein sulfhydryl groups, nor by acting on microtubule-associated proteins. Rotenone and colchicine are competitive inhibitors of tubulin; they appear to bind to the same, or a structurally close, site on tubulin. While the binding of colchicine is essentially irreversible, the binding of rotenone can be reversed by at least two known methods: using the solvent dimethyl sulfoxide and through physical removal by charcoal filtration. *In vitro,* rotenone has been shown to halt mitosis in cancer cells and has not been shown to cause malignancy in normal cells (*4*). However, rotenone does cause mammary fibroadenomas (nonmalignant tumors) in albino rats (*11*).

Information on the mode of action and selectivity of rotenone is important so that it may be used safely and efficiently. Since the three-dimensional structure of most biologically active molecules plays a role in governing their interactions and activities, we report the crystal and molecular structure of rotenone.

EXPERIMENTAL

Rotenone was obtained from the Aldrich Chemical Co., Milwaukee, Wisconsin, and was crystallized by slow evaporation from acetone. Thin, hexagonal, clear yellow crystals appeared in approximately 36 h. No macroscopic degradation due to photochemical reaction was observed over several weeks. Samples kept in the dark did not appear different from those stored in lighted areas. No crystal decay was observed during data collection.

Weissenberg X-ray photographs showed that the space group was $P2_12_12_1$ in the orthorhombic system (*mmm* Laue symmetry, and systematic absences: $h00$, $h = 2n + 1$; $0k0$, $k = 2n + 1$; $00l$, $l = 2n + 1$). After a long search, a suitable crystal with dimensions $0.08 \times 0.26 \times 0.26$ mm was chosen for data collection. The crystal data for rotenone were collected on a Nonius CAD/4 diffractometer with graphite monochromated CuKα (1.5418 Å) radiation. Accurate cell dimensions

TABLE 1

Crystal Data: Rotenone

Empirical formula	$C_{23}H_{22}O_6$
Formula weight	394.43
$F(000)$	1664
Space group	$P2_12_12_1$
Z	8
a	8.413(1) Å
b	19.840(1) Å
c	23.581(1) Å
α	90.0°
β	90.0°
γ	90.0°
V	3936.0 Å^3
D_c	1.331 g cm^{-3}
λCuKα	1.5418 Å
μCuKα	7.038 cm^{-1}
Temperature	approximately 25°C

were obtained from a least-squares fit to the setting angles of 25 reflections chosen widely in reciprocal space in the range 20–25°θ. Intensity data were collected at a variable scan speed ranging from 2 to 30° per minute. Three check reflections were monitored every 100 min of X-ray exposure time. Data were collected in the ω/θ mode (h = 0, 9; k = 0, 22; l = −26, 26)θ: 0–60°. In the shell from θ: 35 to 60°, reflections whose $I < 2\sigma(I)$ were not remeasured at the slow speed. Absorption corrections were calculated from Gaussian quadrature using a grid of 10 × 10 × 10. The 5346 independent data were reduced in the usual manner and averaged to give 2824 unique observations. The R-factor for merging was 0.026. Of these, the 2573 where $F > 2\sigma(F)^2$ were used in subsequent calculations. Crystal data are listed in Table 1.

The structure was solved by direct methods using the program MULTAN (*22*). Several solutions, using 283 E's > 1.5, with high combined figures of merit were chosen to produce E-maps. None of these proved adequate. Upon addition of three new reflections to the starting set, chosen from those appearing at the bottom of the convergence map, and using 332 E's > 1.3, the solution with the lowest residual (27.57) and the highest combined figure of merit (2.81) was chosen to produce an E-map which revealed the position of 55 of the 58 heavy atoms in the asymmetric unit. The remaining three atoms (of the isoprene unit of molecule **I**) were located in a difference map. Initial least-squares refinement revealed high thermal parameters and chemically unacceptable bond lengths and angles for this isoprene unit, although those same atoms in molecule **II** were acceptable. In order to check the appearance of this group, the four atoms constituting this isoprene unit were removed from the model and one cycle of least-squares refinement was

[2] Tables of F_O vs F_C and hydrogen atom positions are available from the authors (M.R.) upon request.

TABLE 2

List of Atomic Coordinates, Isotropic Temperature Factors, and Their Associated Standard Deviations

Molecule 1					Molecule 2				
Atom	*x*	*y*	*z*	*B*	Atom	*x*	*y*	*z*	*B*
C1	1.4074(10)	0.2171(4)	0.6296(4)	5.45(6)	C1′	0.8504(14)	0.0993(5)	0.6580(4)	9.54(9)
O2	1.2489(6)	0.2437(2)	0.6238(2)	4.13(4)	O2′	0.8493(6)	0.0355(2)	0.6900(2)	4.87(5)
C3	1.1493(9)	0.2118(3)	0.5873(2)	3.42(5)	C3′	0.7123(10)	−0.0003(3)	0.6899(3)	4.15(5)
C4	1.1800(9)	0.1526(3)	0.5593(3)	3.94(6)	C4′	0.5806(9)	0.0173(3)	0.6596(3)	3.91(4)
C5	1.0689(10)	0.1260(3)	0.5209(3)	3.72(3)	C5′	0.4441(10)	−0.0229(3)	0.6645(3)	4.32(4)
O6	1.1133(6)	0.0660(2)	0.4963(2)	4.68(4)	O6′	0.3167(6)	−0.0020(2)	0.6306(2)	5.22(5)
C7	0.9931(10)	0.0299(3)	0.4672(3)	4.77(4)	C7′	0.1740(10)	−0.0408(4)	0.6322(4)	6.00(6)
C8	0.8943(9)	0.0793(3)	0.4311(3)	4.29(4)	C8′	0.1981(10)	−0.1130(3)	0.6470(3)	4.65(5)
O9	0.7902(7)	0.0410(2)	0.3965(2)	4.19(4)	O9′	0.2820(6)	−0.1430(2)	0.5995(2)	4.47(5)
C10	0.6555(9)	0.0141(3)	0.4203(3)	3.79(3)	C10′	0.3380(10)	−0.2065(4)	0.6085(3)	4.64(5)
C11	0.5787(9)	−0.0369(3)	0.3913(3)	4.12(4)	C11′	0.3821(9)	−0.2431(3)	0.5617(3)	3.76(4)
C12	0.6067(10)	−0.0676(3)	0.3350(3)	4.65(4)	C12′	0.3861(11)	−0.2263(3)	0.5002(3)	4.73(5)
C13	0.4781(12)	−0.1219(3)	0.3343(3)	5.94(6)	C13′	0.4398(10)	−0.2943(3)	0.4714(3)	4.56(5)
O14	0.3823(7)	−0.1165(2)	0.3851(2)	4.94(4)	O14′	0.4834(7)	−0.3396(2)	0.5211(2)	5.27(4)
C15	0.4455(10)	−0.0670(3)	0.4173(3)	4.09(4)	C15′	0.4420(10)	−0.3110(3)	0.5703(3)	4.21(5)
C16	0.3852(10)	−0.0487(3)	0.4681(3)	4.63(5)	C16′	0.4635(12)	−0.3386(4)	0.6214(4)	5.70(4)
C17	0.4626(9)	0.0049(3)	0.4958(3)	4.06(5)	C17′	0.4177(11)	−0.3015(4)	0.6683(3)	5.13(4)
C18	0.5981(9)	0.0369(3)	0.4726(3)	3.52(5)	C18′	0.3559(10)	−0.2353(4)	0.6640(3)	4.85(4)
C20	0.8056(10)	0.1281(3)	0.4699(3)	3.84(5)	C19′	0.3239(11)	−0.1945(4)	0.7134(3)	5.38(5)
C19	0.6634(10)	0.0956(3)	0.4990(3)	3.81(5)	C20′	0.2899(10)	−0.1207(4)	0.7030(3)	4.90(5)
C21	0.9268(10)	0.1572(3)	0.5115(3)	3.71(6)	C21′	0.4404(10)	−0.0802(3)	0.6984(3)	4.08(4)
C22	0.8936(10)	0.2176(3)	0.5387(3)	4.40(6)	C22′	0.5769(11)	−0.0973(3)	0.7283(3)	4.52(4)
C23	1.0017(9)	0.2463(3)	0.5769(3)	3.67(5)	C23′	0.7160(10)	−0.0587(4)	0.7235(3)	4.58(4)
O24	0.9831(6)	0.3058(2)	0.6057(2)	4.78(5)	O24′	0.8567(7)	−0.0743(2)	0.7473(2)	5.36(5)
C25	0.8368(11)	0.3420(4)	0.5975(4)	6.26(5)	C25′	0.8594(11)	−0.1326(3)	0.7829(3)	5.80(5)
C26	0.3700(20)	−0.1178(8)	0.2851(4)	14.0(1)	C26′	0.3161(9)	−0.3280(3)	0.4370(3)	4.32(4)
C27	0.2729(10)	−0.0765(3)	0.2702(3)	17.2(2)	C27′	0.2358(12)	−0.3811(4)	0.4510(4)	6.80(7)
C28	0.4073(10)	−0.1847(5)	0.2489(5)	15.0(1)	C28′	0.2895(11)	−0.2914(4)	0.3799(3)	5.51(5)
O29	0.6104(6)	0.1195(2)	0.5437(2)	4.78(5)	O29	0.3294(9)	−0.2163(3)	0.7618(2)	7.34(7)

computed. A difference map at this stage was closely examined using interactive graphics (Evans and Sutherland PS330). The electron density was contoured at different levels and no evidence of static disorder was observed even at the lowest level. An attempt was made to model the disorder by including two positions for C27 and C28 (corresponding to rotation about the C13–C26 bond) at partial occupancies in the atom list. This was unsuccessful and the agreement factor increased. We therefore concluded that the best model of the structure was to constrain it to have the dimensions of the chemically identical group of molecule **II.** Hydrogen atoms were placed at at calculated positions (some of these had been observed in difference Fourier maps). The final least-squares refinement using two blocks of parameters (one block for each molecule), with anisotropic temperature factors for all the heavy atoms and isotropic ones for the hydrogen atoms and with isoprene **I** group constrained to have the dimensions of isoprene **II,** converged to an *R*-factor of 0.067. The weighted *R* was 0.072 (number of observations, 2571; number of variables, 518; error of fit, 1.576). A difference map at the conclusion of the refinement showed only two peaks of approximately 0.6 $e/Å^3$ in the vicinity of the isoprene **I** group. In Table 2 are listed the atomic coordinates for the heavy atoms in the two independent molecules. Hydrogen atom coordinates are included in the supplementary material.

Computer programs used were XTAL85 (*23*) and locally written programs (*24*). All diagrams were drawn using VIEW (*25*) and DOCK (*26*).

RESULTS AND DISCUSSION

There are two rotenone molecules in the asymmetric unit and the distances and angles of these molecules agree with those of other molecules having similar atom connectivity. The atomic numbering used in this study and the distances and angles are shown in Fig. 1. Figure 2 illustrates the relationship between molecules in the asymmetric unit. The disorder evident in C26, C27, and C28 could not be sorted out and probably reflects the fact that the two groups substituted on C26 occupy about the same volume; therefore, these groups could occupy either position without disrupting the lattice. The isoprene units are in different orientations in the two molecules. Both molecules **I** and **II** have the C7 *S*, C20 *S*, and C13 *R* configuration. This configuration had been first determined using chemical techniques (*27*) and later confirmed with a brominated rotenone derivative (*28*) using the anomalous dispersion of X-rays from the bromine atom.

The two molecules differ in the way that the two nearly flat regions (rings A and B and rings C, D, and E) are related to each other about the B/C ring junction at C8–C20. The atoms at rings A and B in **I** and **II** can be superimposed, within close limits, with the exception of C8 and C8′ (Fig. 3). Ring B is in a sofa conformation in both molecules, with a slight distortion toward a half-chair in **I**, but with C8 and C8′ on opposite sides of the planar part of the rings. This difference in conformation results in **I** having an extended (linear) shape while **II** is V-shaped. These differences in conformation are illustrated in Fig. 3 and are expressed quantitatively by the torsion angles in the region of the B/C junction (Table 3). Ring C also has opposite conformations in the two molecules (see, for example, the torsion angle O9–C8–C20–C19). The four-coordinate carbon atoms (C8, C20) at the B/C ring junction ensure that even in **I**, the whole molecule is not planar. The angle between the aromatic rings A and D of **I** is 64.3°. These rings are each planar within experimental error in both molecules.

The packing of the two molecules of rotenone is shown in a stereo diagram in Fig. 4. The molecules are able to fit together tightly, maximizing intermolecular interactions; these close contacts are listed in Table 4. The electron-rich carbonyl carbon, O29, of molecule **I** is 3.39(1) Å away from the somewhat positively charged methoxy carbon, C1 of molecule **II**, and 3.282(9) Å from a translationally related C1 of molecule **I**. The shortest contact in the crystal structure occurs between C17 and H12...O6 of translationally related molecules **I**, at a 3.179(9) Å C...O distance.

The tight packing of the rotenone molecules comprising the asymmetric unit provides an explanation for the presence of the two conformations (Fig. 2). Neither two V-shaped molecules nor two of the twisted molecules could pack into such a dense, almost spherical unit. A stacking of only V-shaped molecules would forfeit the interaction advantage gained by placing the carbonyl atoms of one molecule toward electron-poor atoms of another molecule. Similarly, a crystal

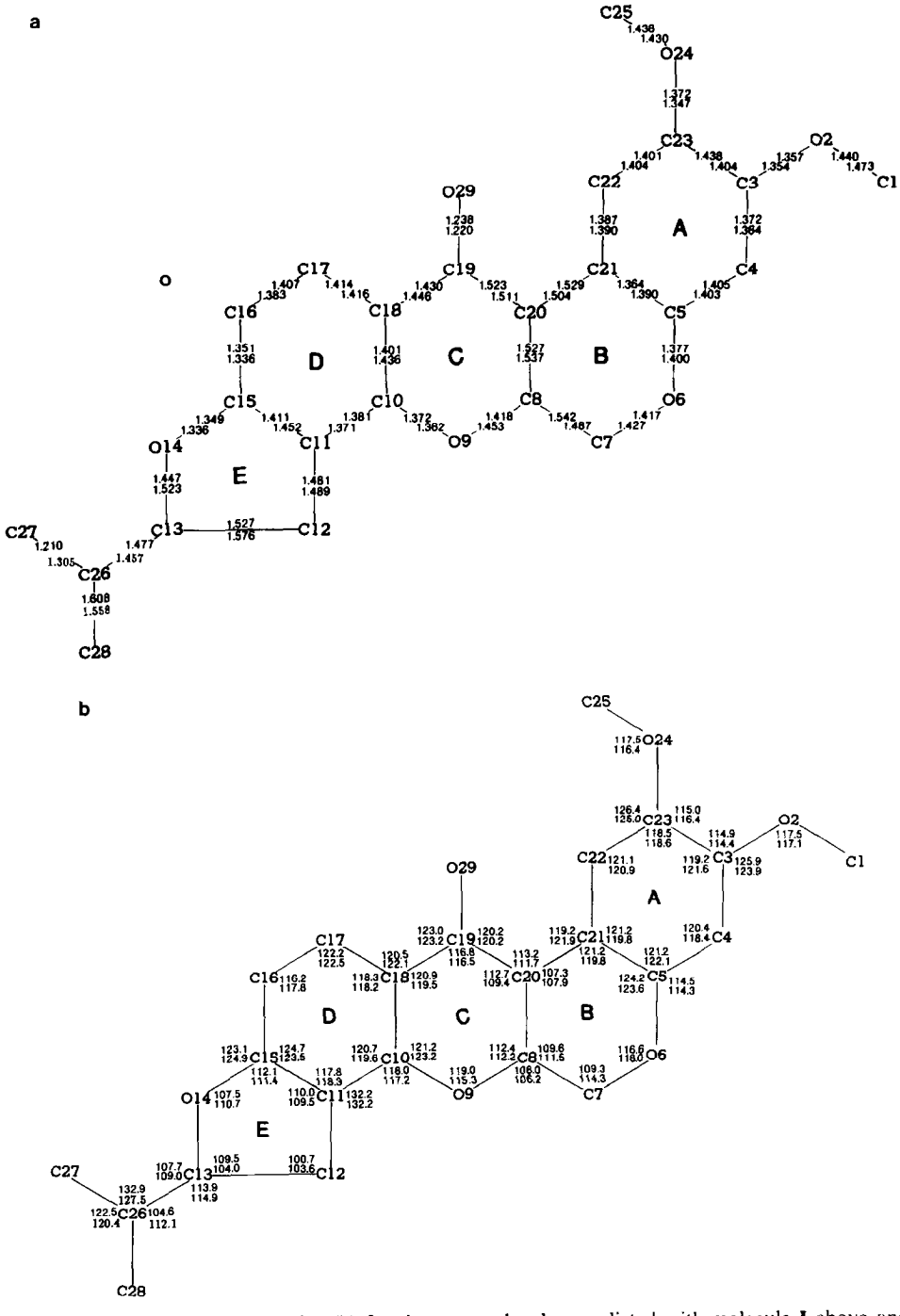

FIG. 1. Distances (a) and angles (b) for the two molecules are listed with molecule **I** above and molecule **II** below. Estimated standard deviations for distances are 0.007–0.010 Å with the exception of the isoprene unit of molecule **I**, whose values for the C26, C27, and C28 and 0.016 Å. The estimated SDs on angle positions are 0.5–0.7° and 1.0° for the angles surrounding the isoprene unit.

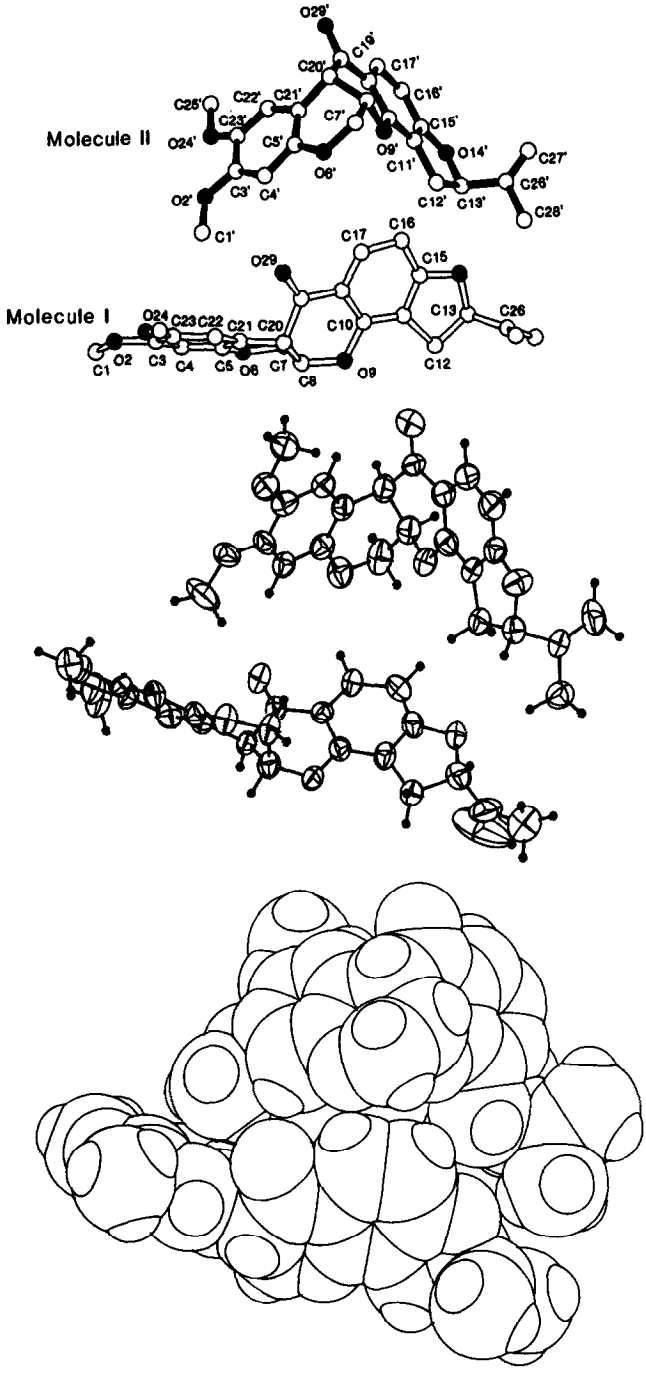

[2]

FIG. 2. The two molecules in the asymmetric unit. The top shows the atomic numbering; the middle shows the same view of the asymmetric unit illustrating the thermal ellipsoids; the bottom shows the van der Waals representation of the asymmetric unit in the same orientation. All three figures are on the same scale; H atoms are included only in the botton two figures. To be noted are the regions of disorder (C26, C27, C28 of molecule I) and the close fit of the two molecules.

TABLE 3

Table of Torsion Angles for Rotenone in the B/C Junction

Atom 1–atom 2–atom 3–atom 4	Molecule 1 angle (°)	Molecule 2 angle (°)
C4–C5–O6–C7	166.6 (6)	178.8 (6)
O6–C7–C8–C20	−65.2 (8)	54.1 (9)
O6–C7–C8–O9	171.9 (6)	−68.4 (8)
C7–C8–O9–C10	77.6 (7)	170.0 (6)
C20–C8–O9–C10	−43.5 (7)	47.8 (8)
C7–C8–C20–C19	−75.0 (8)	−175.0 (7)
C7–C8–C20–C21	50.3 (7)	−53.2 (8)
O9–C8–C20–C19	45.2 (7)	−55.9 (8)
O9–C8–C20–C21	170.5 (5)	65.8 (7)
C18–C19–C20–C8	−22.1 (9)	35.0 (1.0)
C18–C19–C20–C21	−144.2 (6)	−84.4 (9)
O29–C19–C20–C8	157.1 (6)	−147.8 (9)
O29–C19–C20–C21	35.1 (9)	92.7 (1.0)
C8–C20–C21–C5	−18.8 (8)	29.6 (9)
C19–C20–C21–C5	106.2 (7)	149.9 (7)

structure containing only the elongated shape of molecule **I** would prevent a packing arrangement as close and efficient as the one experimentally observed. Thus, the small, but favorable, intermolecular interactions stabilize the two conformers.

Given the presence of the two molecular conformations, it was natural to ask what was the difference in the minimum energy between them. To address this question, molecular mechanics techniques (*29*) were employed. Starting with the fractional coordinates obtained from the diffraction experiment, the compounds were energy minimized. The geometry of the optimized structures was in excellent agreement with that of the experimental structures. The elongated molecule **I**

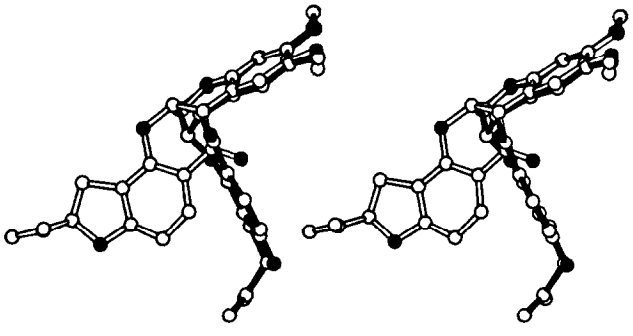

FIG. 3. A stereo view of the two molecules (molecule **II** is shaded) with their A rings superimposed. The two conformations are distinct and the B and C rings are not superimposable.

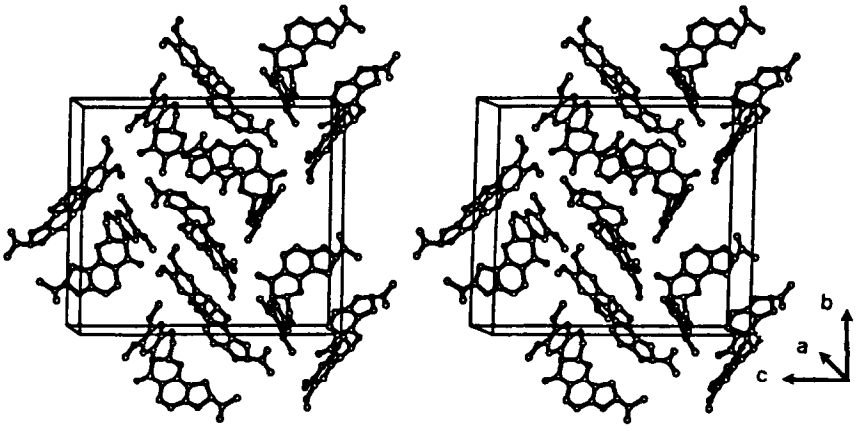

FIG. 4. The packing of the two molecules in the unit cell is illustrated in stereo. Hydrogen atoms have been left off for clarity.

was found to be 5.3 kJ higher in energy than **II**, implying a room-temperature concentration ratio of about 1 : 13 for **I : II**. Although no mention of two conformations has been previously reported even in solution NMR studies, perhaps the resolution of the data was insufficient to detect the minor component. The V-shaped conformation of rotenone has been described (*27, 28, 30, 31*) in solution (proton (*30*) and C-13 NMR studies (*31*)) and solid state studies (*28, 32*). In the crystal structure of the one-to-one complex of rotenone with carbon tetrachloride (*32*), the angle between aromatic rings A and D is 85° (compared with 88.3° in this determination).

The existence of the two conformers of rotenone implies a greater flexibility for the rotenone skeleton than had been appreciated previously. Especially in biologi-

TABLE 4

Close Contacts for Rotenone

	Acceptor	C–H	H...O	C...O	C–H...O angle
C20–H13...O2	$-1/2 + x$, $1/2 - y$, $1 - z$	0.999 (6)	2.463(4)	3.403(7)	156.6(6)
C17–H12...O6	$x - 1$, y, z	1.004 (7)	2.877(5)	3.179(9)	98.1(7)
C25–H17...O6	$-1/2 + x$, $1/2 - y$, $1 - z$	0.998 (9)	2.692(5)	3.430(10)	130.9(6)
C25′–H17′...O9	$3/2 - x$, $-y$, $-1/2 + z$	1.006 (9)	2.644(4)	3.473(9)	139.6(7)
C28′–H20′...O14	x, y, z	0.999 (8)	2.698(4)	3.559(9)	144.6(6)
C20–H13...O24	$-1/2 + x$, $1/2 - y$, $1 - z$	0.999 (6)	2.695(5)	3.502(9)	138.0(8)
C1–H2...O29	$1 + x$, y, z	0.995 (9)	2.595(5)	3.282(9)	126.2(1.1)
C4–H4...O29	$1 + x$, y, z	1.003 (7)	2.809(5)	3.698(9)	148.1(1.1)
C1′–H3′...O29	x, y, z	0.983 (10)	2.578(5)	3.392(12)	140.1(9)
C4′–H4′...O29	x, y, z	1.006 (6)	2.476(5)	3.411(8)	154.5(9)
C7′–H5′...O2′	$x - 1$, y, z	0.997 (9)	2.491(5)	3.407(10)	152.5(7)
C12–H8...O2′	$3/2 - x$, $-y$, $-1/2 + z$	0.997 (6)	2.708(4)	3.498(8)	136.3(7)
C17–H12...O6′	x, y, z	1.004 (7)	2.492(5)	3.411(9)	152.1(6)
C13′–H10′...O9′	$1/2 + x$, $-1/2 - y$, $1 - z$	0.995 (8)	2.778(5)	3.554(9)	135.1(8)
C12′–H8′...O14′	$-1/2 + x$, $-1/2 - y$, $1 - z$	0.999 (9)	2.698(6)	3.666(11)	163.4(7)
C12–H8...O24′	$3/2 - x$, $-y$, $-1/2 + z$	0.997 (6)	2.573(5)	3.507(8)	156.0(6)

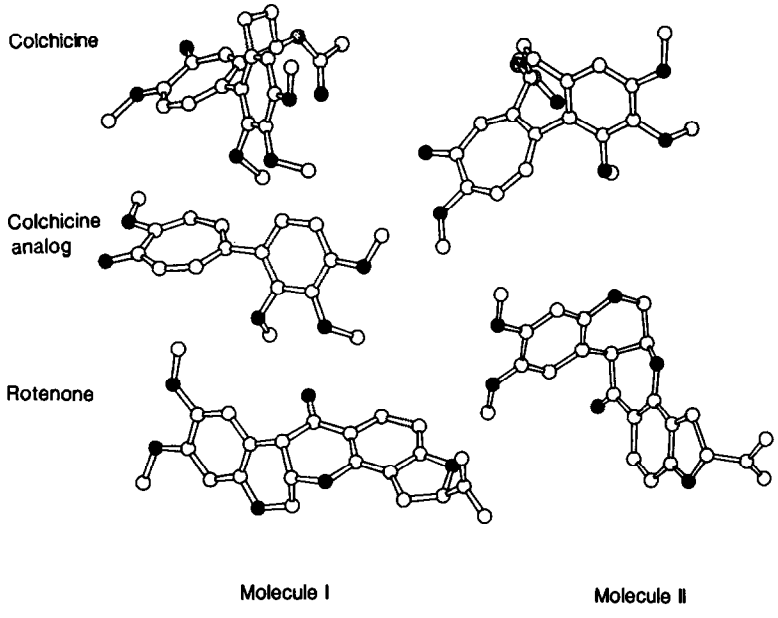

FIG. 5. Crystallographically determined structures of the two molecules in the asymmetric unit of colchicine, the colchicine analog, and the two molecules of rotenone. Hydrogen atoms have been left off.

cal systems, flexibility of molecules is an important factor in the reaction mechanism (e.g., substrate binding to an enzymes). To try and explain rotenone's activity as a mitotic spindle inhibitor, the structures of the tubulin inhibitor colchicine (*33*), a colchicine analog (*34*) (which lacks the central ring of colchicine but is still active), and rotenone were compared. These are shown in Fig. 5. It is known that colchicine is a powerful tubulin inhibitor, while isocolchicine, a structural isomer that has the methoxy and carbonly group positions interchanged on the tropone ring, does not interfere with microtubule assembly. The colchicine analog, despite its freedom to rotate about the bond connecting the two rings (and thus potentially mimicking either colchicine or isocolchicine), assumes a cyrstal structure conformation identical to that of one of the two molecules comprising cholchicine's asymmetric unit. Studies have shown that colchicine is a bifunctional ligand, binding to tubulin both at the tri-methoxy site and the tropone site (*35, 36*). Colchicine derivatives have proved that the tropone site binds strongly to tubulin first, causing a conformational change in the protein, priming it for interaction with the hydrophobic trimethoxy group. Therefore, the experimental observations that isocolchicine, with its rigid framework and the tropone ring substitution reversed from that needed for activity, is inactive, while the more rotationally flexible analog that can assume the colchicine-like orientation is an excellent tubulin inhibitor, are explained.

Rotenone and colchicine are similar at the methoxy-substituted aromatic ring and in their inherent structural flexibility. Despite their fused-ring systems, both

rotenone and colchicine crystallize with two molecules in the asymmetric unit. It is likely that these similarities lead to their similar effects on tubulin.

From this study, it is clear that rotenone has a highly flexible site in the B/C ring junction which manifests itself in the two molecular conformations that make up the asymmetric unit of the crystal. That this junction, particularly the C20 position, is also very chemically reactive is known from an examination of rotenone's metabolic and degradation derivatives. It is clear that this flexibility and reactivity must affect its inhibitory mode of action in the respiratory chain and in mitosis, although the actual mechanism is not known. More complete studies need to be done to better characterize the nature of the many functions of rotenone.

ACKNOWLEDGMENTS

The authors gratefully acknowledge the help and support of the members of the crystallographic laboratories at ICR, particularly Dr. J. Glusker and Dr. H. Berman for the use of equipment. From Flinders University, we thank Dr. C. Schiesser for help with the use of the MM2 program and Dr. M. Thompson for useful conversations and are grateful for a visiting research fellowship grant to M.R. This research was supported by National Science Foundation Grant R11-8300122 and Grant 16970-GB4 Type G of the Petroleum Research Fund of the American Chemical Society to M.R. In addition, American Cancer Society Grants BC-132 and BC-242, National Institutes of Health Grants CA-10925 and CA-27780, and an appropriation from the Commonwealth of Pennsylvania were responsible for the diffractometer and computer equipment used at the Institute for Cancer Research in Philadelphia.

REFERENCES

1. WARE, G. W. (1983) Pesticides Theory and Application, Freeman, San Francisco.
2. MCEWEN, F. L., AND STEPHENSON, G. R. (1979) The Use and Significance of Pesticides in the Environment, Wiley, New York.
3. GOSALVEZ, M. (1983) *Life Sci.* **32,** 809–816.
4. HALEY, T. J. (1978) *J. Environ. Pathol. Toxicol.* **1,** 315–337.
5. CARSON, R. L. (1962) Silent Spring, Fawcett Crest, New York.
6. O'BRIEN, R. D. (1967) Insecticide Action and Metabolism, Academic Press, New York/London.
7. FUKAMI, J.-I., YAMAMOTO, I., AND CASIDA, J. (1967) *Science* **155,** 713–716.
8. ENGSTROM-HEG, R., AND COLESANTE, R. T. (1979) *N.Y. Fish Game J.* **26**(1), 22–36.
9. NEWSOME, W. H., AND SHIELDS, J. B. (1980) *J. Agric. Food. Chem.* **28**(4), 722–724.
10. LOFFLER, M., AND SCHNEIDER, F. (1982) *Mol. Cell. Biochem.* **48,** 77–90.
11. GOSALVEZ, M., DIAZ-GIL, J., ALCANIZ, J., AND BORRELL, J. (1979) *Biochem. Soc. Trans.* **7,** 113–115.
12. KOSHIDA, M., TAKENAKA, A., OKAMURA, H., AND MORI, T. (1987) *J. Reprod. Fertil.* **79,** 391–395.
13. ASHACK, R. J., MCCARTY, L. P., MALEK, R. S., GOODMAN, F. R., AND PEET, N. P. (1980) *J. Med. Chem.* **23,** 1022–1026.
14. LEBER, A. P., AND PERSING, R. L. (1979) U. S. NTIS PB Rep. PB-290, p. 962.
15. LEBER, A. P., AND THAKE, D. C. (1979) U. S. NTIS PS Rep. PS-79, 0976, p. 18.
16. GUTMAN, M., SINGER, T. P., BEINERT, H., AND CASIDA, J. E. (1970) *Proc. Natl. Acad. Sci. USA* **65**(3), 763–770.
17. PALMER, G., HORGAN, D. J., TISDALE, H., SINGER, T. P., AND BEINERT, H. (1968) *J. Biol. Chem.* **243**(4), 844–847.
18. BOIS, R., AND ESTABROOK, R. W. (1969) *Arch. Biochem. Biophys.* **129,** 362–369.

19. GONDAL, J. A., AND ANDERSON, W. A. (1986) *J. Biol. Chem.* **260,** 12690–12694.
20. MEIJER, M., SCHUITENMAKER, M. G., BOOGERD, F. C., WEVER, R., AND STOUTHAMER, A. H. (1978) *Arch. Microbiol.* **119,** 119–127.
21. MARSHALL, L. E., AND HIMES, R. H. (1978) *Biochim. Biophys. Acta* **543,** 590–594.
22. MAIN, P., FISKE, S. J., HULL, S. E., LESSINGER, L., GERMAIN, G., DECLERCQ, J.-P., AND WOOLFSON, M. M. (1978) MULTAN Computer Program.
23. STEWART, J. M., AND HALL, S. R. (1983) XTAL System of Crystallographic Programs, University of Maryland, College Park.
24. CARRELL, H. L. (1978) Crystallographic Programs, The Institute for Cancer Research, Philadelphia.
25. CARRELL, H. L. (1977) VIEW, The Institute for Cancer Research, Philadelphia.
26. STODOLA, R. K., MANION, F. J., AND WOOD, W. P. (1986) DOCK, The Fox Chase Cancer Center, Philadelphia.
27. BUCHI, G., CROMBIE, L., GODIN, P. J., KALTENBRONN, J. S., SIDDALINGAIAH, K. S., AND WHITING, D. A. (1961) *J. Chem. Soc.*, 2843–2860.
28. BEGLEY, M. J., CROMBIE, L., WHITING, D. A. (1975) *J. Chem. Soc. Chem. Commun.*, 850–851.
29. ALLINGER, N. L. (1977) MM2, QCPE No. 395, 423 version.
30. CARLSON, D. G., WEISLEDER, D., AND TALLENT, W. H. (1973) *Tetrahedron* **29,** 2731–2741.
31. CROMBIE, L., KILBEE, G. W., AND WHITING, D. A. (1975) *J. Chem. Soc. Perkin Trans. I,* 1497–1499.
32. ARORA, S. K., BATES, R. B., GRADY, R. A., AND DELFEL, N. E. (1975) *J. Amer. Chem. Soc.* **97**(20), 5752–5755.
33. LESSINGER, L., AND MARGULIS, T. N. (1978) *Acta Crystallogr.* **B34,** 578–584.
34. ROSSI, M., LINK, J., AND LEE, J. C. (1984) *Arch. Biochem. Biophys.* **231**(2), 470–476.
35. ANDREU, J. M., AND TIMASHEFF, S. N. (1982) *Biochemistry* **21,** 6565–6576.
36. ANDREU, J. M., AND TIMASHEFF, S. N. (1982) *Biochemistry* **21,** 534–543.